

Unearthing modes of climatic adaptation in underground storage organs across Liliales

Carrie M. Tribble^{1,*}, Michael R. May^{2,3,4}, Abigail Jackson-Gain^{2,3,5}, Rosana Zenil-Ferguson¹, Chelsea D. Specht⁶, and Carl J. Rothfels^{2,3}

¹*School of Life Sciences, University of Hawai'i at Mānoa, Honolulu, HI, 96822, USA*

²*Department of Integrative Biology University of California, Berkeley, CA 94709, USA*

³*University Herbarium, University of California, Berkeley, CA 94709, USA*

⁴*Department of Evolution and Ecology, University of California, Davis, CA 95616, USA*

⁵*Current address: Departamento de Geología, Facultad de Ciencias Físicas y Matemáticas, Universidad de Chile, Santiago, Chile*

⁶*Section of Plant Biology and L.H. Bailey Hortorium, School of Integrative Plant Sciences, Cornell University, Ithaca, NY 14853 USA*

Abstract Testing adaptive hypotheses about how continuous traits evolve in association with developmentally-structured discrete traits, while accounting for the confounding influence of other, hidden, evolutionary forces, remains a challenge in evolutionary biology. In one example of this, geophytes are herbaceous plants capable of retreating underground and use underground storage organs (USOs) to survive extended periods of unfavorable conditions. Such plants have evolved multiple times independently across all major vascular plant lineages. Even within closely related lineages, however, geophytes show impressive variation in the morphological modifications and structures (i.e., “types” of USOs) that allow them to survive underground. Despite the developmental and structural complexity of USOs, the prevailing hypothesis is that they represent convergent evolutionary “solutions” to a common ecological problem, though some recent research has drawn this into question. We extend existing phylogenetic comparative methods to test for links between geophytes’ hierarchical discrete morphological traits associated with USOs and adaptation to environmental variables, using a phylogeny of 621 species in Liliales. We found that plants with different USO type do not differ in climatic niche more than expected by chance, with the exception of root morphology, where modified roots are associated with lower temperature seasonality. These findings suggest that root tubers may reflect adaptations to different climatic conditions than those represented by other types of USOs. Thus, the tissue type and developmental origin of the USO structure may influence the way it mediates ecological relationships, which draws into question the appropriateness of ascribing broad ecological patterns uniformly across geophytic taxa. This work provides a new framework for testing adaptive hypotheses and for linking ecological patterns across morphologically varying taxa while accounting for developmental (non-independent) relationships in morphological data. [Macroevolution, geophytes, climatic niche evolution, adaptation]

Introduction

1 The evolution of major innovations in life history strategies (how organisms gather and store energy and reproduce)
2 is one of the primary themes of biodiversity research (Adler et al., 2014; Enquist et al., 1999). However, such studies
3 are often limited by methodological challenges in integrating distinct datatypes into a single analytical framework (see
4 Theoretical Overview, below). In this work, we build on recent advances in modeling complex, structured discrete traits
5 and the adaptive evolution of continuous traits; we develop an analytical pipeline for testing adaptive hypotheses
6 about the evolution of life history strategies.

7 In one remarkable example of a life history innovation, certain herbaceous plants can retreat underground by pro-
8 ducing the buds of new growth on structures below the soil surface (Raunkiaer et al., 1934), while also storing nutri-
9 ents to fuel this growth in highly modified, specialized underground storage organs (USOs). Such “geophytes” have
10 evolved independently many times across the plant tree of life, including in diverse and distantly related lineages
11 within the ferns and flowering plants (Tribble et al., 2021). Even within closely related lineages, geophytes show re-
12 markable variation in the particular morphological modifications that allow them to survive underground. By differen-
13 tially modifying leaves, stems, or roots, geophytes produce complex storage structures through distinct developmental
14 and evolutionary means (reviewed in Tribble et al., 2021). For example, plants may produce bulbs by modifying leaves
15 for storage; rhizomes, corms, and stem tubers by modifying stem tissue; and root tubers by modifying root tissue.

16 Previous work has suggested that the geophytic habit is correlated with distinct abiotic features—specifically, more
17 seasonal climatic conditions and higher-disturbance regimes (Patterson and Givnish, 2002; Cuéllar-Martínez and Sosa,
18 2016; Sosa et al., 2016; Sosa and Loera, 2017; Howard et al., 2019)—and may be an adaptation to these conditions (Rees,
19 1989). Supporting this conclusion, geophytes are particularly diverse in seasonally dry climates such as Mediterranean
20 ecosystems, where they survive hot, dry summers underground and emerge during cool, wet winters to photosynthe-
21 size and reproduce, a pattern particularly prominent in the Cape region of South Africa, where almost 15% of native
22 plant species are geophytic (Parsons and Hopper, 2003). Geophytes are also common in deciduous woodland habitats,
23 where their USOs fuel quick spring regrowth to maximize photosynthetic opportunities before trees have leafed-out in
24 spring (Whigham, 2004). One of the first studies to test for a correlation between niche and USO type (Patterson and
25 Givnish, 2002) found that within Liliaceae, plants with bulbs occupy more open and seasonal habitats than plants with
26 rhizomes. In a recent study of monocotyledonous geophytes, Howard et al. (2019) found similar patterns: geophytism
27 is correlated with areas of lower temperature and precipitation and higher temperature variation. Howard et al. (2019)
28 also tested for distinct climate preferences among geophytes with different types of USOs; they found no significant
29 correlations with the exception of an association between rhizomatous geophytes and areas of increased temperature
30 variation. The authors suggest that more detailed morphological data, as well as data related to the developmental
31 origin of USOs (leaf, stem, or root tissue), may be necessary to address variation within geophytes in environmental
32 preferences.

33 If geophytes with independently evolved and developmentally distinct morphologies converge on the same cli-
34 matic niche, then the diverse types of USOs may represent different evolutionary paths towards an effectively similar
35 ecological strategy: retreating underground. This result would imply that the diversity of underground forms are due
36 to developmental or genetic constraints that predisposed plants to modify particular types of tissue in different ways
37 when presented with the same types of environmental conditions. Conversely, if plants with different USOs occupy dif-
38 ferent climatic niches, variation in underground morphology may underlie important differences in how these plants
39 relate to their environment. In this case, geophytism may not be a uniform life-history strategy at all; rather, each
40 distinct morphology may represent a specific adaptive response to a particular set of abiotic conditions. To date, no
41 study has explicitly tested if geophytes with different USOs are adapted to particular climatic niches within an adaptive
42 evolutionary framework that accommodates complex hierarchical relationships between geophyte morphologies.

43 Representation of diverse geophytic morphologies is particularly high in the monocot order Liliales, which con-
44 tains roughly 1200 species distributed across the globe (Givnish et al., 2016; Patterson and Givnish, 2002), including
45 geophytic taxa with a striking diversity of USOs. In this study, we infer a species-level phylogeny of roughly 50% of
46 the taxa in Liliales by capitalizing on the growing availability of published genetic data (Benson et al., 2018), advances
47 in supermatrix construction (de Queiroz and Gatesy, 2007), and model-based tree-building algorithms (Ronquist et al.,
48 2012), which collectively have widened the scope of phylogenetic reconstruction and allow for the inference of increas-
49 ingly large trees that can provide the statistical power to test complex adaptive scenarios. We use this phylogeny and a
50 newly-developed analysis pipeline to test the relationship between underground morphologies and adaptive evolution
51 of climate seasonality.

52 **Theoretical Background**

53 While the goal of many phylogenetic comparative methods is to model the evolutionary relationships between (often
54 multiple) traits and species, incorporating diverse data types into a cohesive analytical framework is often stymied
55 by underlying differences in how distinct types of traits are expected to evolve across a tree. Specifically, including
56 continuous and discrete traits in a single analysis is a longstanding challenge. Some previous approaches to correlate
57 discrete and continuous traits include the use phylogenetic generalized linear models (Garland Jr et al., 1993) and the
58 threshold model (Felsenstein, 2012). However, these methods are purely correlative and do not account for the presence
59 of other, hidden, evolutionary forces that could cause morphological change (Beaulieu et al., 2013; Uyeda et al., 2018).

60 The Ornstein-Uhlenbeck (OU) process is defined by three parameters: σ^2 , θ , and α (Hansen, 1997; Butler and King,
61 2004). As with Brownian Motion (BM), a trait evolving under the OU process experiences random changes with mean
62 zero and a magnitude proportional to the rate parameter, σ^2 . However, unlike BM, a trait evolving under OU is also
63 subject to deterministic changes: it is “pulled” toward the optimal value θ , approximating the evolution of the trait
64 toward an adaptive peak. The strength of the pull is proportional to α and the distance from the optimum, such
65 that traits that are far away from the optimum are pulled more strongly (the so-called “rubber-band” effect). Further

66 elaboration of the OU process may allow the parameters to vary across the branches of a phylogenetic tree (Beaulieu
67 et al., 2012; Uyeda and Harmon, 2014). In these models, optima may themselves evolve across the phylogeny (Uyeda
68 and Harmon, 2014), unlinked to any observed discrete character. Alternatively, users may specify the location of the
69 multiple optima across the tree (Beaulieu et al., 2012), perhaps based on estimated ancestral states. However, this type
70 of explicit link between trait(s) and adaptive optima attributes all variation in the optima to the discrete trait and may
71 lead to a spurious correlation. It is therefore necessary to incorporate additional sources of adaptive-optima evolution
72 or to allow for imperfect correspondence between the discrete trait and continuous regimes.

73 Furthermore, some types of USOs may share greater affinities in morphological and developmental space because
74 they are modifications of the same type of tissue. For example, in both corms and rhizomes, stem tissue is modified
75 for storage, while in bulbs, the primary storage tissue is derived from modified leaves (see Figure 1). A model that
76 represents transitions between corms and rhizomes in the same way that it represents transitions between rhizomes
77 and bulbs effectively erases the complexity of these morphologies and ignores the role that shared developmental
78 mechanisms may play in morphological disparification. Tarasov et al. (2019) presented a novel pipeline—PARAMO—
79 to incorporate developmental hierarchies into discrete ancestral-state estimation using hidden states and structured
80 Markov models (See also Tarasov, 2019). In PARAMO, character states are expanded or combined and hierarchical
81 relationships are expressed by disallowing transitions between certain combinations of character states and requiring
82 transitions through intermediate character states (i.e., using structured, hidden Markov models). Often, these hierar-
83 chies are based on ontological definitions, though similar information on character state structure can be incorporated
84 without formal ontologies. This approach addresses the red tail/blue tail problem (Lee and Bryant, 1999): how does
85 one code tail color for a species with no tail? Thus, the PARAMO pipeline is appropriate for modeling the evolution
86 of complex morphologies, where some species may have modifications to certain tissues/ body parts while others lack
87 those modifications or tissues altogether. As such, PARAMO provides a coherent way to model changes in morpho-
88 logically distinct USOs, such that the type of tissue modified to produce the USOs influences what transitions between
89 structures are allowed. For example, PARAMO models the evolution of rotund root tubers independently from the
90 evolution of rhizomes, as these structures are modifications of different parts of the plants (root and stem, respectively).

91 Below, we describe our approach to testing the effect of a discrete, morphological trait on the adaptive evolution of
92 a continuous trait while accounting for the nuances presented above.

93 **Materials and Methods**

94 To test if plants with the same type of USO are evolving towards a shared optimal climatic niche, we developed an
95 analytical pipeline based on recent advances in trait evolution models. We independently model the evolution of dis-
96 crete and continuous traits. For the discrete trait (USOs), we use a model of morphological evolution that accounts
97 for complex nested relationships among characters (PARAMO, Tarasov et al., 2019). For the continuous trait (climatic
98 niche), we use comparative methods that allow for explicit testing of adaptive hypotheses (bayou; Uyeda and Harmon,

99 2014). Both these methods produced histories (maps) of trait evolution over a phylogeny, so we then combine these
100 maps to test for correspondence between the traits' evolutionary histories. Finally, we compare this combined history
101 with one produced under a null model (where there is no relationship between USOs and climate). This procedure
102 allows us to test for correlations between USO evolution and climatic niche evolution while accounting for hierarchi-
103 cal structure in morphological data produced by developmental processes, the complex adaptive landscape of climatic
104 niche evolution, and the potential effects of hidden evolutionary forces influencing continuous trait evolution.

105 **Data**

106 We generated three data sets for downstream analysis: a distribution of species-level phylogenies including 50% of the
107 species in Liliales; a modeled climatic niche for each species based on 19 climatic variables (Fick and Hijmans, 2017);
108 and a detailed underground morphology database for all species.

109 **Phylogeny**

110 We used SUMAC 2.0 (Freyman, 2015) to download gene regions from NCBI GenBank (Benson et al., 2018) for all
111 species in the order Liliales. We targeted genes that clustered with specific guide sequences to obtain sequences for
112 10 commonly sequenced genes in Liliales (Table S.1). We filtered the resulting sequences using custom Python scripts
113 to remove regions that were recovered from fewer than 150 taxa out of the 621 taxa available on GenBank, to remove
114 sites with more than 95% missing data, and to align sequences. All regions were aligned using MAFFT v7.271 (Katoh
115 and Standley, 2013); some alignments (ITS, psbA, and rpl16, and trnL-trnF spacer) failed to align well under MAFFT
116 and were subsequently aligned using PASTA (Mirarab et al., 2015) to improve alignment accuracy. We concatenated
117 the filtered and edited alignments using Sequence Matrix (Vaidya et al., 2011). We reconstructed the phylogeny using
118 MrBayes v3.2.6 (Ronquist et al., 2012) on CIPRES (Miller et al., 2011) with two independent runs of four chains, par-
119 titioned by gene region, each under the GTR + Γ model with default priors (Table SS.2). We constrained tree space to
120 enforce family-level monophyly and monophyly of the non-parasitic clade (all Liliales families except Campynemat-
121 aceae and Corsiaceae) according to the Angiosperm Phylogeny Website (Stevens et al., 2016), to reduce run times.

122 To account for phylogenetic uncertainty, we performed all downstream analyses on a random set of ten trees from
123 this posterior distribution (see section *Sensitivity of Results to Tree Selection*). We dated each of the selected trees in R (R
124 Core Team, 2013) using the `chronos()` function from the `ape` package (Paradis and Schliep, 2019)—an implementation
125 of the penalized-likelihood approach (Sanderson, 2002)—using data from two fossils and a secondary calibration (see
126 Table S.3; Iles et al., 2015; Givnish et al., 2016). We set $\lambda = 1$ (the smoothing parameter).

127 **Climate**

128 We modeled the climatic niche of each sampled species using a newly developed R pipeline, Climate and Niche Dis-
129 tribution Inference (CaNDI, available at <https://github.com/abbyj-g/candi>) that gathers and cleans species occur-

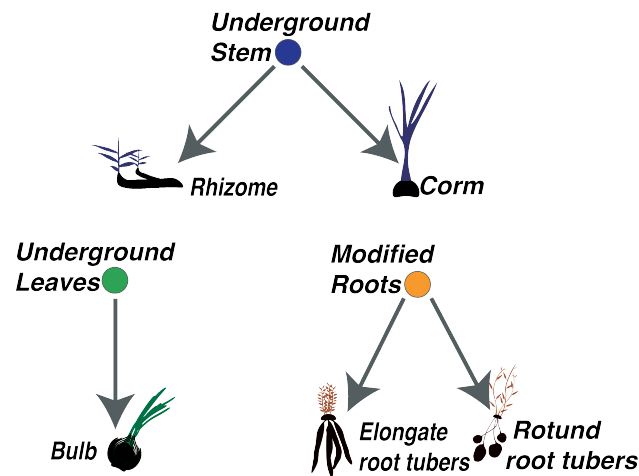


Figure 1: Hierarchy of morphological states used in PARAMO analysis.

130 rences, downloads climate data, and estimates niches for hundreds of taxa at a time. CaNDI takes as input a list of
131 species, queries the Global Biodiversity Information Facility (GBIF; Flemons et al., 2007) and the Botanical Information
132 and Ecology Network (BIEN Maitner et al., 2018) for occurrence records, and cleans those records using a series of
133 filters designed to remove latitude and longitude records that fall outside of the species' native range, are exactly at 0°,
134 90°, or 180°, or are in the ocean. CaNDI then passes these occurrence points and their associated climate data to MaxEnt
135 (Phillips and Dudík, 2008) to estimate the climatic niche. For each species, CaNDI returns the probability of occurrence
136 across the landscape.

137 For the climate data we used 19 bioclimatic variables from the WorldClim database (Fick and Hijmans, 2017), which
138 describe various aspects of temperature and precipitation. Collinearity of predictor variables does not affect model
139 performance (except in cases of model transfer; Feng et al., 2019), so we included all 19 variables in niche estimation.
140 From the niche reconstructions we calculated a single estimate of the optimal value for each climate variable by selecting
141 the value that corresponded to the part of the species' range with the highest probability of occurrence. Downstream
142 analyses focused on the two axes of the multidimensional niche that describe seasonality: seasonality of precipitation
143 and seasonality of temperature.

144 **Morphology**

145 We used morphological data from Kew's World Checklist of Selected Plant Families (WCSP; WCSP, 2020) to describe
146 the USOs associated with each sampled species. For taxa listed as tuberous, we referred to morphological literature
147 (Kubitzki and Huber, 1998; Sanso and Xifreda, 2001; Pate and Dixon, 1982) for more detailed descriptions, as the WCSP
148 uses tuber as a catch-all category, encompassing corms, root tubers, and other organs. The final coding scheme consisted
149 of the presence and absence of eight characters, grouped into three hierarchical clusters based on tissue type (leaf, stem,
150 and root; see Figure 1).

151 **Analysis**

152 We integrated the climate data, morphology data, and phylogeny in a novel analysis pipeline that integrates newly-
153 developed methods for modeling continuous characters (such as climate) and discrete characters (such as morphologi-
154 cal categories). This pipeline models the continuous and discrete variables independently, and then asks if variation in
155 adaptive optima for continuous characters are explained by the state of the discrete trait, allowing for complex models
156 of the discrete trait and for an imperfect correspondence between adaptive optima and the discrete trait.

157 **Climatic Niche Evolution**

158 We used the R package *bayou* (Uyeda and Harmon, 2014) to describe the modes of evolution of climatic niche in Liliales
159 across each of ten phylogenies sampled from the posterior of our phylogenetic analysis; *bayou* models the evolution of
160 a continuous character under an OU process (Butler and King, 2004), allowing for the optimum of the OU process to
161 vary across the branches of the phylogeny (Uyeda and Harmon, 2014). Specifically, this approach models the number
162 and placement of adaptive regimes across the branches of the phylogeny, where each adaptive regime is characterized
163 by a unique optimal continuous-trait value, θ , rate of evolution, σ^2 , and strength of selection, α . These regimes and their
164 associated parameter values are sampled in proportion to their posterior probabilities using reversible-jump MCMC
165 (Green, 1995).

166 For both temperature and precipitation seasonality we log-transformed the variable and ran *bayou* for 3.5 million
167 generations using the priors specified in Table S.4. Priors were selected as recommended in the *bayou* tutorial (Uyeda,
168 2019) except for the prior on k (number of θ s), which we modified to reflect our uncertainty in k . The recommended
169 prior on k is a Poisson distribution with $\lambda = 10$. However, we opted for a geometric distribution with $p=1/30$, which
170 is equivalent to setting an exponential hyperprior on λ and increasing the expected value of λ from 10 to 30. We
171 assessed convergence using the R package *coda* (Plummer et al., 2006) and based on those results discarded the first
172 1% of samples as burnin. We drew 1000 samples (maps) from the posterior distribution of adaptive regimes for each
173 climatic niche variable to use in subsequent calculations. Each of these samples contains a history of adaptive-optima
174 evolution, which maps the adaptive optima along branches of the phylogeny.

175 **Morphological Evolution**

176 We used the PARAMO pipeline (Tarasov et al., 2019) to reconstruct the evolution of underground morphologies using
177 hidden, structured Markov models and stochastic mapping across the ten trees used in our *bayou* analyses. Under-
178 ground morphologies are not adequately represented in published ontologies (Tribble et al., 2021; Howard et al., 2021),
179 so instead of using ontologies to determine the hierarchical relationships between states, we built a dependency matrix
180 of USOs based on the type of tissue modified for storage (Figure 1). PARAMO uses hidden states that represent the
181 “predisposition” to evolve USOs of different tissue types (Beaulieu et al., 2013), incorporating the hierarchy of states
182 illustrated in Figure 1. Each cluster (leaf, stem, and root) corresponds to a distinct evolutionary model such that the

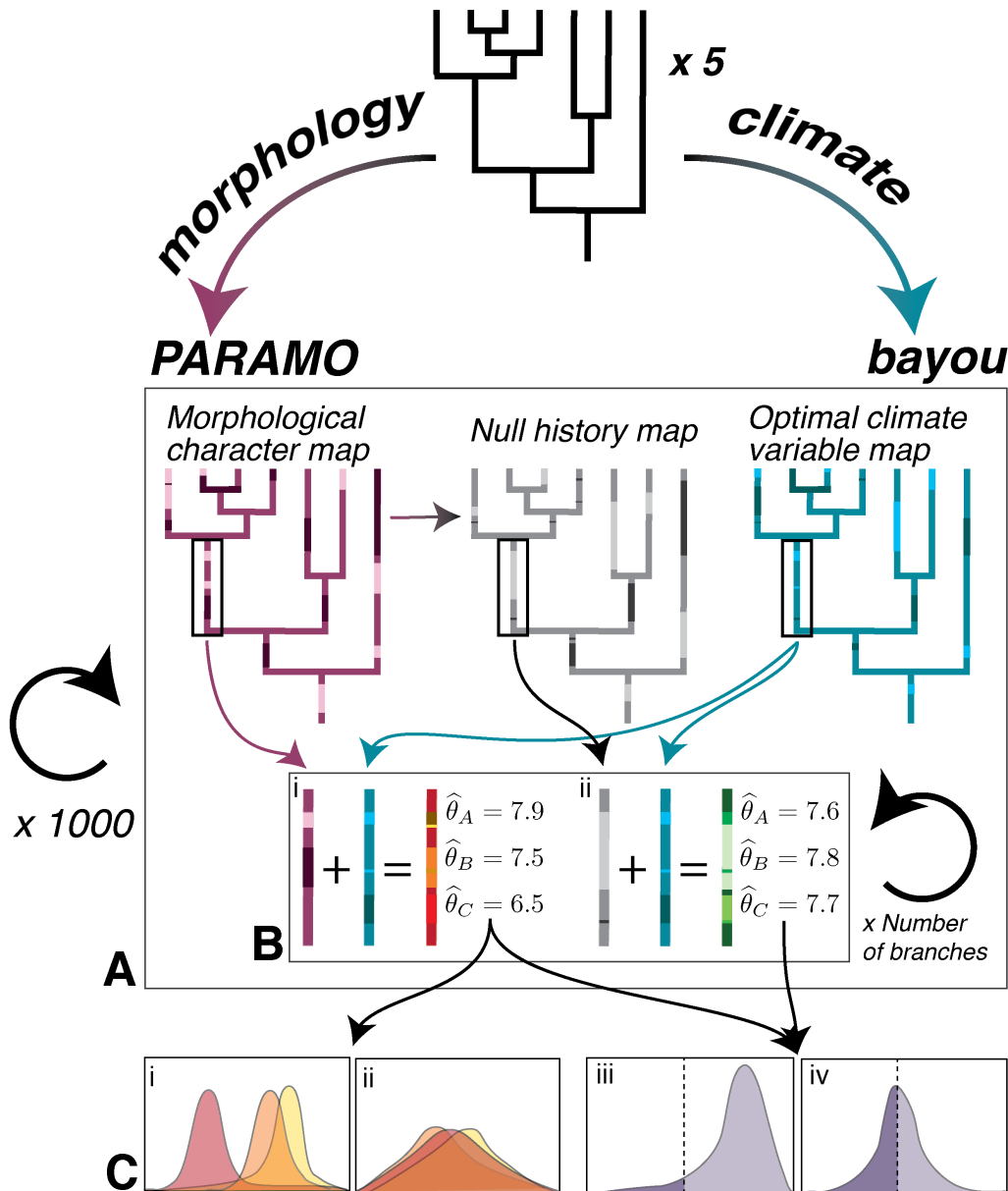


Figure 2: Schematic representation of methods used in this study. For each of ten phylogenies sampled from the posterior distribution, we: A) used PARAMO and bayou to generate 1000 stochastic maps of the morphology and estimated climatic niche optima, individually, and to simulate 1000 null histories (see Methods: Hypothesis testing) using the estimated evolutionary models from PARAMO. B) We combined each of the niche optima maps with a morphological character map, and separately with a null history map, to create two sets of state-specific optimum maps that show the state-specific $\hat{\theta}_j$ parameters per character state. C) We plot the densities of all estimated state-specific $\hat{\theta}_j$ parameters (i, ii) and the distribution of a test statistic (iii, iv; see Methods: Hypothesis testing). Plots i and iii represent a case where we would reject the null model, while in plots ii and iv we would fail to reject the null.

183 clusters evolve independently. First, for each of the three clusters, we estimated evolutionary transition rates between
184 character states using the R package corHMM (Beaulieu et al., 2013). We then reconstructed their evolutionary histories
185 by simulating the evolution of each cluster under the inferred model of evolution and conditioning on the observed
186 data at the tips (i.e., stochastic mapping, Nielsen, 2002; Huelsenbeck et al., 2003) using the `make.simmap()` function
187 in `phytools` (Revell, 2012). Each morphological stochastic map represents one possible scenario of character evolution
188 under the inferred model. We then made a single “combined phenotype” morphological map by overlaying the maps
189 of each cluster. The combined phenotype map illustrates the history of the entire underground phenotype with many
190 character states. We repeated this process 1000 times to produce 1000 combined phenotype maps to capture uncertainty
191 in the history of each cluster.

192 **Calculating State-Specific Climatic Optima**

193 The previous steps have produced N bayou maps and N morphological maps (where $N = 1000$ in this study). Each
194 morphological map defines a set of breakpoints where the state changes; likewise, each bayou map defines a set of
195 breakpoints where the climatic optimum changes. We use the i^{th} bayou map and the i^{th} morphological map to produce
196 a state-specific-optimum map, such that each branch on the tree can be represented as a set of segments and where each
197 segment corresponds to a particular combination of morphological state and climatic optimum (Figure 2B). For a given
198 state-specific-optimum map, we compute the average climatic optimum for a given morphological state j as:

$$\hat{\theta}_j = \frac{1}{\tau_j} \sum_{k \in T_j} \theta_k,$$

199 where T_j is the set of all segments in morphological state j , τ_j is the sum of lengths of segments in T_j , and θ_k is the
200 climatic optimum associated with segment k . We repeat this procedure for each of the N state-specific-optimum maps,
201 producing a posterior distribution of state-specific average climatic optima, $\hat{\theta}_j$.

202 As the observed morphology rather than the hidden states are expected to affect an organism’s relationship to its
203 environment, we collapsed the full set of character states (observed and hidden) into the observed states by combining
204 the state-dependent optima of states with the same observed state but different hidden states. Some states were visited
205 infrequently during stochastic mapping and thus had high percentages of missing data (i.e., were rarely inferred as an-
206 cestral states across the 1000 maps), which made estimates of their state-specific optima more uncertain. To avoid these
207 uncertain estimates, we dropped from analysis those states represented in less than 50% of the maps. We performed
208 these comparisons for both precipitation and temperature seasonality and for the three morphological clusters (leaf,
209 stem, and root) and the combined morphological phenotype, for a total of eight comparisons.

210 **Hypothesis Testing: Climate and Morphological Trait Correlation**

211 Our null hypothesis is that plants with different USOs are not evolving towards different climatic niche optima; in other
212 words, that state-specific climatic niche optima ($\hat{\theta}_j$) are equal. Correspondingly, under the alternative hypothesis, state-

specific $\hat{\theta}_j$ are different. However, for any finite dataset, inferred state-specific $\hat{\theta}_j$ values will be different, even under the null hypothesis, and this issue is exacerbated by the phylogenetic structure of the inferred $\hat{\theta}_j$ values. To account for this structure, and the finite sample, we calculated a test statistic (defined below) that summarizes the overall difference between any particular set of state-specific $\hat{\theta}_j$. We simulated the distribution of that test statistic under the null model and checked whether the differences generated under the null model were significantly less than the differences of the empirical estimates.

We simulated 1000 null histories of the three characters (leaf, stem and root) using the `sim.history()` function in the Rpackage `phytools` (Revell, 2012) and the estimated Q-matrices from the empirical analyses. This procedure differs from stochastic mapping in the empirical analysis in that the simulations are not conditioned on the observed character data. As in the empirical analysis, we also combined the three characters to produce 1000 null histories of the combined phenotype. This null model represents the case where a discrete trait evolves under the same evolutionary model as the observed discrete trait, but without the observed pattern at the tips. Any correspondence between the simulated traits and climate is due to chance, the distribution of the climate data on the tree, and/or the rates of evolution and stationary frequencies of the model, rather than the distribution of morphological states across the tree.

To calculate the test statistic, for a given vector of state-specific $\hat{\theta}_j$ values, we calculated the pairwise distance between all state-specific $\hat{\theta}_j$. These distances represent the extent to which character states are linked to different estimated $\hat{\theta}_j$; in other words, the optimal climatic values differ between discrete states. These distances result in a distance matrix, D (for a simple two-state example):

$$D = \begin{pmatrix} d(\hat{\theta}_1, \hat{\theta}_1) & d(\hat{\theta}_1, \hat{\theta}_2) \\ d(\hat{\theta}_2, \hat{\theta}_1) & d(\hat{\theta}_2, \hat{\theta}_2) \end{pmatrix}$$

where $d(\hat{\theta}_l, \hat{\theta}_m)$ is the distance between $\hat{\theta}_l$ and $\hat{\theta}_m$:

$$d(\hat{\theta}_l, \hat{\theta}_m) = \sqrt{(\hat{\theta}_l - \hat{\theta}_m)^2}.$$

We then measure the overall amount of difference using the Frobenius norm, $F(D)$, which summarizes the magnitude of the distance matrix. For a given bayou map i , we calculate S_i , the difference between $F(D_i)$ given the stochastic map and $F(D_i)$ given the null history. We then compute S_i for each bayou sample; if 0 is in the 95% probability interval of S , we do not reject the null model.

Sensitivity of Results to Phylogenetic Uncertainty

We performed all the above analyses on ten trees randomly sampled from the posterior distribution of our phylogenetic analysis. To determine if our results were sensitive to particularities of the sampled trees, we analyzed each tree individually and two sets of five trees each. While the results vary by individual tree (Figure S1), sampling at least five trees is sufficient to produce consistent results (Figure S2); the results do not change meaningfully between either

241 analysis of five trees or the full analysis of ten trees (Figures 5 and S2), so we present results based on the combined ten
242 trees.

243 **Data and Code Availability**

244 All code is freely available on GitHub: https://github.com/cmt2/underground_evo and all data will be made avail-
245 able on Dryad prior to publication.

246 **Results**

247 Across all ten trees, the ancestor of Liliales is estimated to have had a rhizome with no leaf or root modifications
248 (Figure 3 A–D shows the reconstructions for one tree), in agreement with previous work (Patterson and Givnish, 2002;
249 Howard et al., 2019). For both temperature and precipitation seasonality, the estimated optima at basal branches in the
250 phylogeny are highly seasonal, with subsequent shifts into less seasonal optima along more recent branches (Figure 3
251 E and F).

252 Figure 4 illustrates the distribution of estimated state-specific optima. Overall, the distributions of state-specific
253 optima are more dispersed across the temperature seasonality axis than the precipitation seasonality axis. For the
254 leaf cluster, the estimated averaged optima for bulb-bearing plants are more seasonal than those for no bulb. For the
255 stem cluster, plants with either rhizomes or corms are estimated to be associated with reduced seasonality than plants
256 without stem modification, though for precipitation only rhizomes are estimated to be less seasonal than the other
257 states. In the root cluster, plants with root tubers (especially rotund root tubers) have lower temperature seasonality
258 than those without root tubers, but for precipitation, plants with rotund root tubers and without root tubers overlap in
259 their distributions while plants with elongate root tubers are estimated to be more seasonal. In the combined phenotype
260 for temperature, the most seasonal state for precipitation is plants with both bulbs and rhizomes and the least seasonal
261 state is plants with rhizomes and rotund root tubers. For precipitation seasonality in the combined phenotype, most
262 state-specific optima have highly overlapping distributions, though it appears that plants with rhizomes are slightly less
263 seasonal and plants with rhizomes and elongate root tubers are slightly more seasonal than other distributions. For both
264 temperature and precipitation, the distribution corresponding to no modified underground organs (non-geophytes)
265 falls out intermediate along both climatic niche axes and overlaps with many other states, signifying that non-geophytes
266 are not more or less seasonal than geophytes.

267 While the state-specific optima curves in Figure 4 appear distinct for many of the morphology-climate comparisons,
268 across both climate variables, no distributions are more different than expected by chance (P-values 0.216–0.626), with
269 the exception of the root cluster for temperature seasonality, which is significant (P-value 0.044; Figure 5).

Climatic adaptation in underground organs

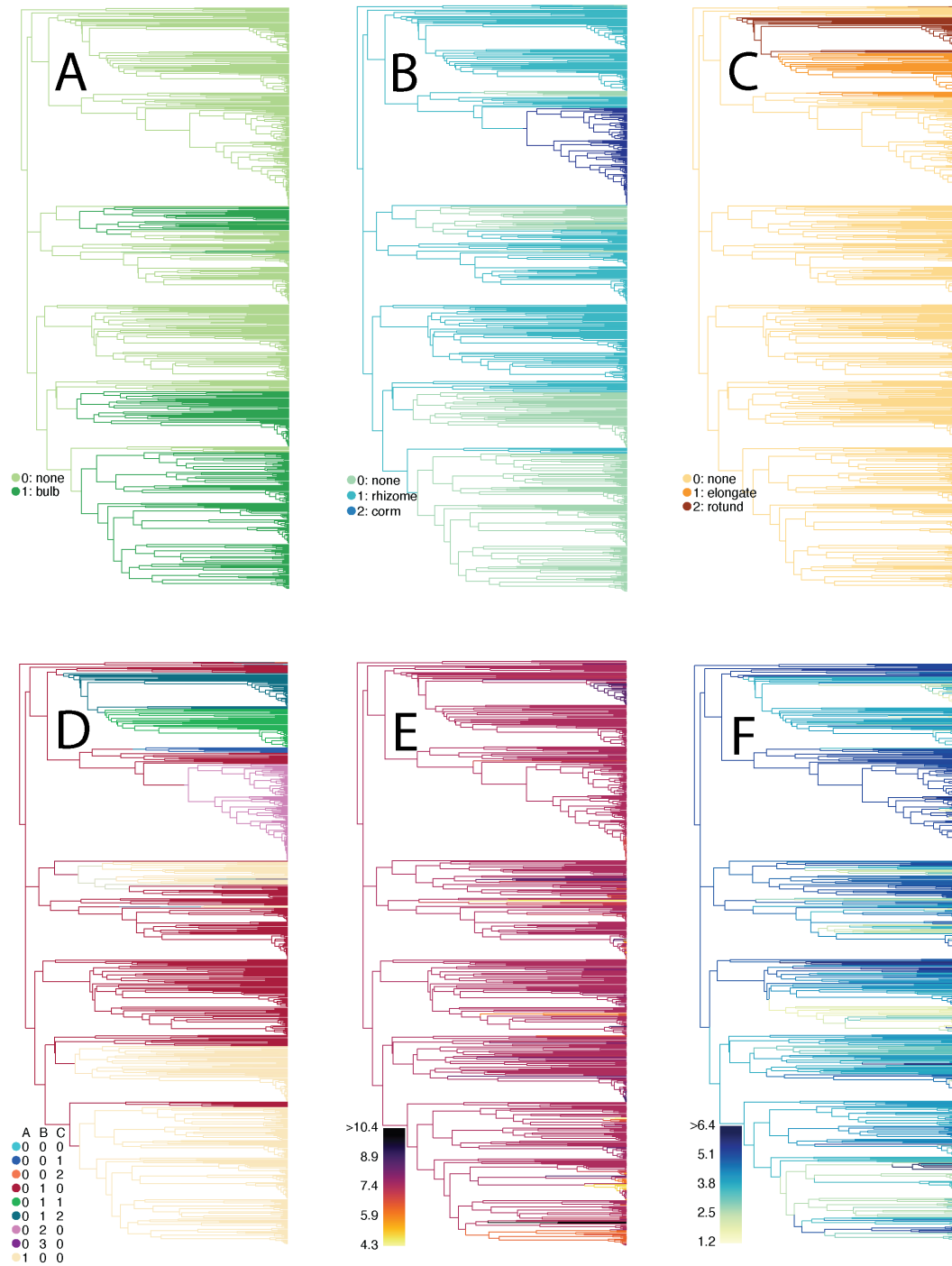


Figure 3: Stochastic maps of estimated ancestral states for one of five trees used in the analysis: A) leaf character map showing inferred evolutionary history of having or not having a bulb, B) map of estimated history of stem modifications, C) map of estimated evolutionary history of root modifications, D) combined phenotype character produced by amalgamating maps A-C, E) posterior mean branch-specific θ for temperature seasonality, F) posterior mean branch-specific θ for precipitation seasonality. In A, B, and C, the “none” category applies to absence of modifications of the relevant tissue type; those taxa may have modifications of the other tissues.

Climatic adaptation in underground organs

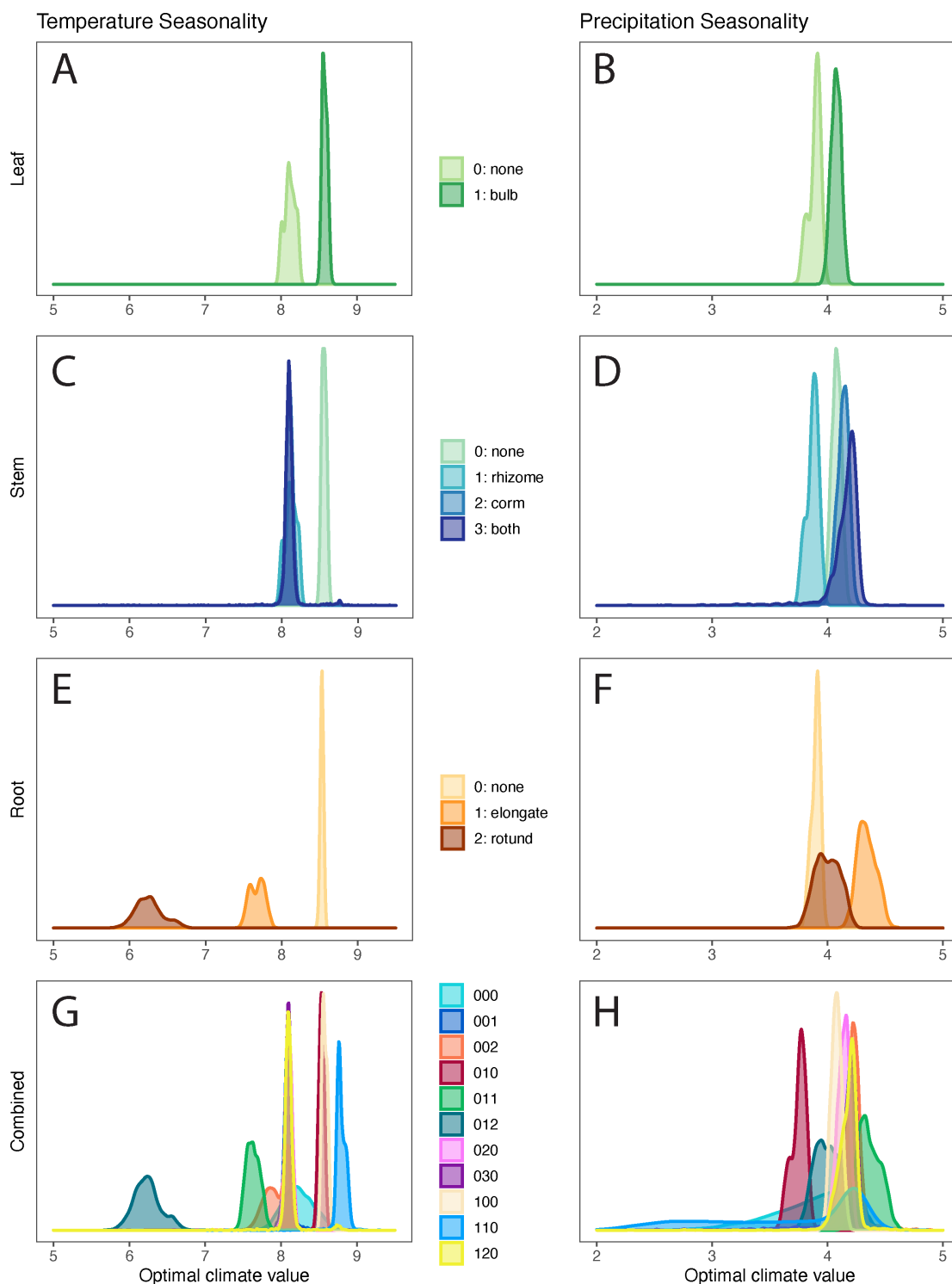


Figure 4: Posterior distributions of state-specific $\hat{\theta}$ parameters. Panels A, C, E, and G depict $\hat{\theta}$ distributions for temperature seasonality, while panels B, D, F, and H show $\hat{\theta}$ distributions for precipitation seasonality. A — B refer to the leaf cluster, C — D to the stem cluster, E — F to the root cluster, and G — H to the combined phenotype. For these combined phenotype densities (G — H), digits in the state labels refer to states for each cluster. The first digit corresponds to the leaf state, the second digit corresponds to the stem state, and the third digit corresponds to the root state. For example, the 000 state refers to the absence of any USO, and 012 refers to a geophyte with rhizomes and rotund root tubers.

Climatic adaptation in underground organs

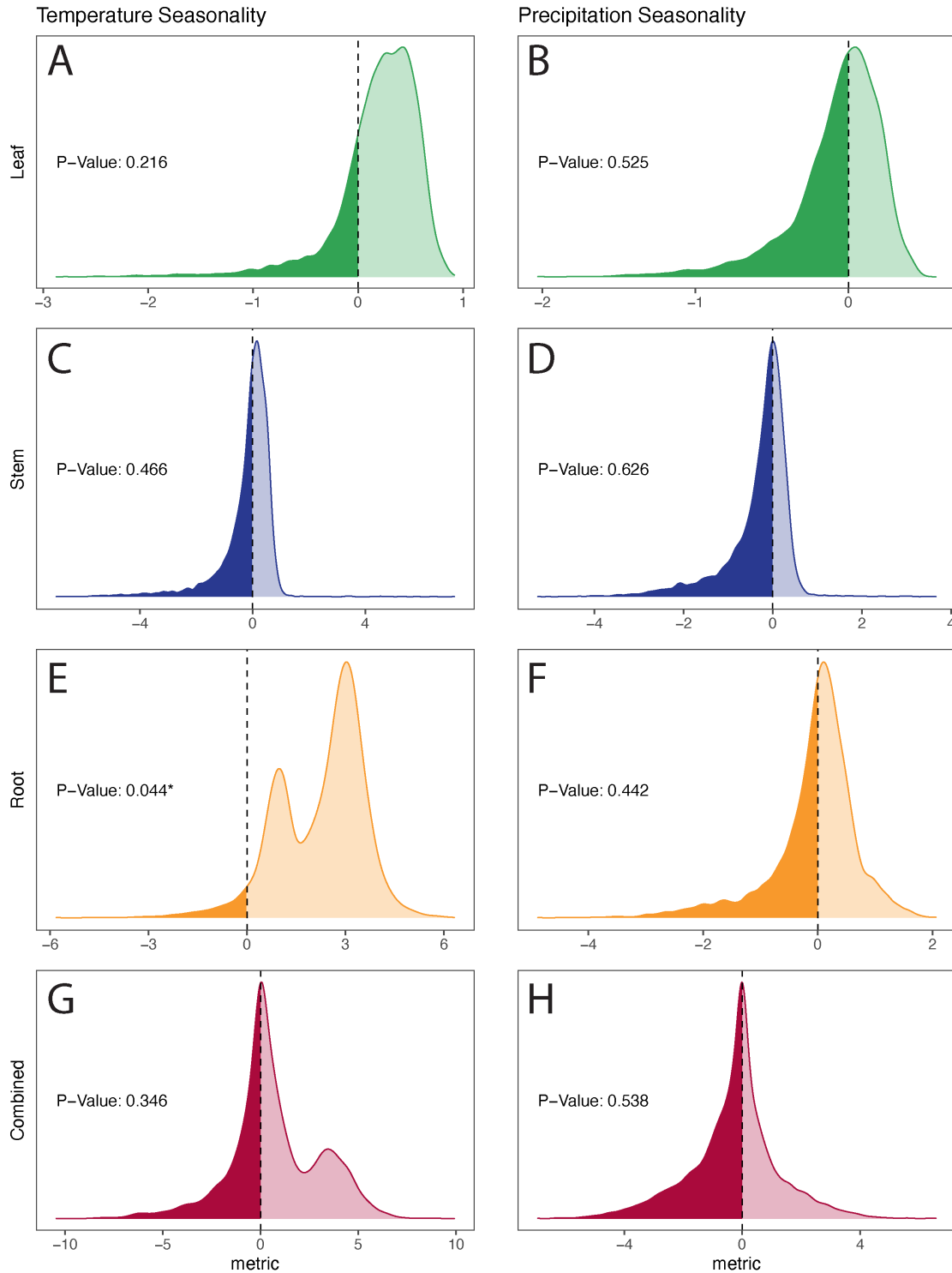


Figure 5: Test statistic (S) distributions. Panels A, C, E, and G depict S distributions for temperature seasonality, while panels B, D, F, and H show S distributions for precipitation seasonality. A — B refer to the leaf cluster, C — D to the stem cluster, E — F to the root cluster, and G — H to the combined phenotype. Distributions with 95% > 0 are considered evidence for a statistically significant difference in state-specific $\hat{\theta}$. P-Values correspond to the percent of values equal to or less than zero. Of all comparisons, only root and temperature seasonality are statistically significant (panel E).

270 Discussion

271 Applicability of analysis pipeline for future comparative studies

272 This work demonstrates the utility of applying complex evolutionary models to address a long-standing challenge in
273 statistical comparative biology: modeling relationships among discrete and continuous traits. Some implementations
274 of OU models allow for continuous traits to evolve under regimes dictated by the evolutionary history of discrete traits
275 (such as implemented in OUwie, Beaulieu et al., 2012); an important advancement in these methods allows for modeling
276 a hidden character with a fixed number of states, thus including hidden variation in the evolution of the continuous
277 trait (Vasconcelos et al., 2021). However, these approaches impose potentially restrictive assumptions on the number
278 of adaptive regimes associated with either hidden or observed traits.

279 Our analytical pipeline unites three main components. First, we use PARAMO (Tarasov et al., 2019) to estimate the
280 evolutionary history of a discrete trait while taking into account hierarchical relationships between character states. Sec-
281 ond, we use bayou (Uyeda and Harmon, 2014) to estimate the number and location of adaptive regimes of continuous-
282 trait evolution that best fit the data. Third, our pipeline combines these estimates by calculating the average optimal
283 values for each discrete trait and asks if these averaged optima are more different from each other than expected under
284 a null model.

285 This pipeline has several advantages over existing methods. First, the model parameters have clear biological in-
286 terpretations. Densities from Figure 4 show the distributions of probable optimal phenotypes ($\hat{\theta}_j$) of the continuous
287 trait by discrete category. These $\hat{\theta}_j$ correspond to peaks in the adaptive landscape of the continuous trait, so the esti-
288 mated parameter values have a clear and direct link to evolutionary theory, unlike the estimated effect sizes from linear
289 models. Second, the method directly models the evolutionary process of the discrete traits and thus is appropriate
290 for addressing evolutionary dependence between continuous and discrete traits. This contrasts with methods such as
291 phylogenetic ANOVA, which treat discrete tip states as purely a source of nonrandom structure at the present, rather
292 than actually modeling the evolution of the trait across the tree. Third, the pipeline can accommodate a wide variety of
293 models for the evolution of the discrete traits. We use PARAMO (Tarasov et al., 2019) to model the nested relationships
294 among USOs derived from the same tissue. In some empirical cases, not including the present study, traits are explicitly
295 defined in ontologies (e.g., phenoscape.org), and PARAMO uses these definitions directly to establish the hierarchy
296 between character states. As the use of ontologies in comparative biology becomes more common, incorporating hi-
297 erarchies codified in ontologies will greatly expand the ability of researchers to test increasingly complex hypotheses,
298 including how developmental processes impact trait evolution and the relationships among traits (Howard et al., 2021).
299 However, any model of discrete trait evolution that can produce simulated character histories can also generate stochas-
300 tic map histories, and thus could be used instead of PARAMO. For example, one could produce stochastic maps from
301 a state-dependent speciation and extinction (SSE) analysis (BiSSE, for example, Maddison et al., 2007), and thus link
302 discrete ancestral states, informed by variable speciation and extinction rates, to a continuous character of interest.

303 Finally, this method allows for imperfect correspondence between the estimated optimal continuous trait and the
304 discrete states. The evolution of continuous traits in general, and climatic niches in particular, is complex and almost
305 certainly explained by many other variables beyond those that are targeted for analysis. It is thus inappropriate to force
306 our model to test between either no correspondence or full correspondence between the continuous-trait evolution
307 and the state of a focal discrete trait. SSE methods may provide a useful analogy; the addition of hidden states allow
308 these models to apportion the variation in speciation and extinction rates between the observed trait of interest and an
309 unobserved hidden trait (Rabosky and Goldberg, 2015; Beaulieu and O’Meara, 2016). Similarly, our method examines
310 the distributions of state-dependent optima without requiring that the continuous trait regimes and the discrete trait
311 vary perfectly together over the tree. We test for significance by comparing these observed distributions to distributions
312 that are built from our null expectation of random evolution of the discrete trait. We thus avoid the “straw-man effect”
313 described in May and Moore (2020), in which any variation in the process of continuous-trait evolution is spuriously
314 attributed to the discrete trait, because the null hypothesis is that there is no variation at all.

315 All code and scripts used in this pipeline are publicly available at https://github.com/cmt2/underground_evo.

316 **Getting at the root of the problem: are USOs adaptations to particular climatic niches?**

317 We used this pipeline to test for correlated evolution between climatic seasonality and geophytic USOs. These analyses
318 demonstrate that plants in Liliales with the same underground storage organ do not occupy different climatic niches
319 more than expected by chance, with the exception of root morphology, where the presence of modified roots, especially
320 rotund root tubers, is associated with lower temperature seasonality. Furthermore, non-geophytes in Liliales are not
321 associated with more or less seasonal climates than their geophytic counterparts. While many of the state-specific
322 optima curves appear distinct (Figure 4), the null model suggests that these differences could be observed even with
323 no correspondence between the trait and climate (Figure 5), due to the phylogenetic structure of environmental niche
324 preference in the underlying data.

325 These findings suggest that root tubers may be an adaptation to distinct ecological conditions or that root-tuber-
326 bearing taxa experience physiological constraints that restrict them to particular climatic niches, unlike the other geo-
327 phytes included in this study. Root tubers are also unique morphologically among the USOs included in this study;
328 unlike corms, rhizomes, and bulbs, root tubers—especially in Liliales—are rarely the source of perennating under-
329 ground buds. Most geophytes in Liliales with root tubers also have rhizomes (e.g., *Bomarea*, *Alstroemeria*), which may
330 serve as the source of underground buds while the root tubers store nutrients and water (Tribble et al., 2021). Many
331 geophytes regenerate their USOs annually (especially bulbs and corms; Pate and Dixon, 1982; Kamenetsky and Okubo,
332 2012), and thus the processes of nutrient flow between the USO and the above-ground plant are necessarily linked to
333 the same seasonal cycles. Partitioning growth and storage between organs (as in the case of the species with tubers
334 and rhizomes) may be particularly advantageous in climates with less temperature seasonality, as it allows for the con-
335 tinuous production of aerial shoots and the periodic replacement of stored nutrients as needed. Alternatively, places

336 with less seasonal temperatures may be less likely to reach the freezing point, and root tubers may be particularly
337 maladapted to frost compared to USOs derived from stem or leaf tissue.

338 The results of our study differ from previous work in three primary ways. First, while we found no significant
339 difference in the environmental niche of geophytes and non-geophytes, prior work suggested that geophytes are as-
340 sociated with lower temperatures and precipitation and higher temperature variation compared with non-geophytes
341 (Howard et al., 2019). Because of the sparse representation of non-geophytes in Liliales, our dataset may lack sufficient
342 power to detect generalizable patterns of climatic niche occupancy between geophytes and non-geophytes. Secondly,
343 previous work found that rhizomes are correlated with increased temperature variation and found no evidence for
344 different niches between tuberous and non-tuberous taxa (Howard et al., 2019), while our analysis found no significant
345 association between rhizomatous or non-rhizomatous taxa but instead suggests that taxa with root tubers evolve to-
346 wards lower optimal values of temperature seasonality. These differences may be due to the scale of the study; Howard
347 et al. (2019) aimed to identify monocot-wide patterns, but our study focuses a smaller taxonomic scale, and is able to
348 investigate patterns of morphological evolution in greater detail. Of particular note, the Howard et al. (2019) study
349 does not distinguish between root tubers and stem tubers, and thus would not have been able to recover the associa-
350 tion between roots and lower temperature seasonality that we find here. Thus, our results illustrate the importance of
351 detailed “development-aware” character coding in comparative studies.

352 Thirdly, Patterson and Givnish (2002) found evidence that in the core Liliales, convergence on bulbs correlated with
353 independent transitions into seasonal and high-light habitats, but while we also find evidence for several independent
354 transitions to bulbs, the association between bulbs and increased seasonality is not statistically significant in our results
355 (P-values 0.216 and 0.525 for temperature seasonality and precipitation seasonality respectively). The Patterson and
356 Givnish (2002) study was one of the first to address geophyte evolution in a phylogenetic framework and correlated
357 storage organs with discrete habitat types, but recent advances in statistical phylogenetics have made more nuanced
358 approaches possible, such as our new pipeline. Specifically, our study uses continuous climatic data directly in the
359 analysis, rather than discrete habitat categories, and employs a coherent model of adaptive continuous trait evolution. It
360 is possible that discrete habitat categories obscured important variation in seasonality, leading to a spurious correlation
361 between seasonality and the presence of bulbs.

362 In Liliales, root tubers are mostly restricted to a few clades (namely *Bomarea*, *Alstroemeria*, *Burchardia*, and a few ad-
363 ditional taxa), so it is possible that the strong association between decreased temperature seasonality and the presence
364 of root tubers is driven by an unmeasured trait that happens to co-occur in those clades. For this reason, extrapo-
365 lating our results to non-liliid geophytes may not be appropriate, and follow-up studies should address variation in
366 root morphology and climate in other clades, particularly in groups with many independent transitions between the
367 absence and presence of root tubers and between different root tuber morphologies. *Asparagus* would be a particu-
368 lar appropriate system in which to further test these associations, as root morphology is highly variable in the genus
369 (Leebens-Mack, pers. comms.). However, there are few other clades known for well-characterized variation in the
370 presence and absence of root tubers or for variation in root tuber morphology. Underground morphology is vastly

371 under-characterized in many plant clades (Tribble et al., 2021; Janzen et al., 1975), so this work also motivates increased
372 morphological characterization of USOs and root morphology in particular, and demonstrates the importance of con-
373 tinued emphasis on classic botanical techniques for understanding biodiversity. In addition, studies that characterize
374 the functional ecology and physiology of root tubers will likely yield important insights into how and why they differ
375 from other USOs.

376 Conclusions

377 This study introduces an analysis pipeline that infers the relationship between adaptive optima for a continuous trait
378 and the hierarchical, nested evolution of a discrete trait, controlling for other factors driving changes in adaptive optima.
379 While previous methods have attempted to address this issue, ours is the first that allows the number of adaptive
380 regimes to vary in a way that best fits the data. This pipeline is applicable across many areas of evolutionary biology
381 and may serve as a model for future hypothesis-driven comparative research. Our pipeline can accommodate an
382 array of complex models of discrete morphological trait evolution (such as models that account for the developmental
383 history of morphological traits) into tests of correlated trait evolution, and implements a novel approach to account
384 for imperfect correspondence between adaptive regimes and discrete traits. These advances are key steps forward as
385 ecological and evolutionary studies increasingly seek to incorporate the nuance and complexity of natural variation
386 into quantitative models that permit formal hypothesis testing.

387 Author Contributions

388 CMT designed and executed the study. CMT collected data. CMT and AJ-G performed analyses, and MRM advised on
389 statistics. CMT, MRM, CJR, CDS, and RZ-F guided interpretation of results.

390 Acknowledgements

391 We would like to acknowledge Benjamin K. Blackman, David D. Ackerly, and members of the Rothfels Lab *sensu lato*
392 at UC Berkeley for valuable feedback on earlier versions of the manuscript. Conversations with Cody Coyotee Howard
393 and Jesus Martínez-Gómez guided treatment of underground storage organs and interpretation of results. Josef C.
394 Uyeda provided advice on implementing PARAMO without relying on formal ontologies. This is publication number
395 xxx from the School of Life Sciences at UHM.

396 References

397 Adler, P. B., Salguero-Gómez, R., Compagnoni, A., Hsu, J. S., Ray-Mukherjee, J., Mbeau-Ache, C., and Franco, M. (2014). Functional
398 traits explain variation in plant life history strategies. *Proceedings of the National Academy of Sciences*, 111(2):740–745.

Climatic adaptation in underground organs

- 399 Beaulieu, J. M., Jhwueng, D.-C., Boettiger, C., and O'Meara, B. C. (2012). Modeling stabilizing selection: expanding the ornstein-
400 uhlenbeck model of adaptive evolution. *Evolution: International Journal of Organic Evolution*, 66(8):2369–2383.
- 401 Beaulieu, J. M., O'Meara, B. C., and Donoghue, M. J. (2013). Identifying hidden rate changes in the evolution of a binary morphological
402 character: the evolution of plant habit in campanulid angiosperms. *Systematic Biology*, 62(5):725–737.
- 403 Beaulieu, J. M. and O'Meara, B. C. (2016). Detecting hidden diversification shifts in models of trait-dependent speciation and extinc-
404 tion. *Systematic Biology*, 65(4):583–601.
- 405 Benson, D. A., Cavanaugh, M., Clark, K., Karsch-Mizrachi, I., Ostell, J., Pruitt, K. D., and Sayers, E. W. (2018). Genbank. *Nucleic acids*
406 *research*, 46(D1):D41–D47.
- 407 Butler, M. A. and King, A. A. (2004). Phylogenetic comparative analysis: a modeling approach for adaptive evolution. *The American*
408 *Naturalist*, 164(6):683–695.
- 409 Cuéllar-Martínez, M. and Sosa, V. (2016). Diversity patterns of monocotyledonous geophytes in Mexico. *Botanical Sciences*, 94(4):699.
- 410 de Queiroz, A. and Gatesy, J. (2007). The supermatrix approach to systematics. *Trends in ecology & evolution*, 22(1):34–41.
- 411 Enquist, B. J., West, G. B., Charnov, E. L., and Brown, J. H. (1999). Allometric scaling of production and life-history variation in vascular
412 plants. *Nature*, 401(6756):907–911.
- 413 Felsenstein, J. (2012). A comparative method for both discrete and continuous characters using the threshold model. *The American*
414 *Naturalist*, 179(2):145–156.
- 415 Feng, X., Park, D. S., Liang, Y., Pandey, R., and Papeş, M. (2019). Collinearity in ecological niche modeling: Confusions and challenges.
416 *Ecology and evolution*, 9(18):10365–10376.
- 417 Fick, S. E. and Hijmans, R. J. (2017). WorldClim 2: new 1-km spatial resolution climate surfaces for global land areas. *International*
418 *journal of climatology*, 37(12):4302–4315.
- 419 Flemons, P., Guralnick, R., Krieger, J., Ranipeta, A., and Neufeld, D. (2007). A web-based GIS tool for exploring the world's biodiver-
420 sity: The Global Biodiversity Information Facility Mapping and Analysis Portal Application (GBIF-MAPA). *Ecological informatics*,
421 2(1):49–60.
- 422 Freyman, W. A. (2015). SUMAC: Constructing phylogenetic supermatrices and assessing partially decisive taxon coverage. *Evolution-*
423 *ary Bioinformatics*, 11:EBO–S35384.
- 424 Garland Jr, T., Dickerman, A. W., Janis, C. M., and Jones, J. A. (1993). Phylogenetic analysis of covariance by computer simulation.
425 *Systematic Biology*, 42(3):265–292.
- 426 Givnish, T. J., Zuluaga, A., Marques, I., Lam, V. K., Gomez, M. S., Iles, W. J., Ames, M., Spalink, D., Moeller, J. R., Briggs, B. G.,
427 et al. (2016). Phylogenomics and historical biogeography of the monocot order Liliales: out of Australia and through Antarctica.
428 *Cladistics*, 32(6):581–605.
- 429 Green, P. J. (1995). Reversible jump Markov chain Monte Carlo computation and Bayesian model determination. *Biometrika*, 82(4):711–
430 732.
- 431 Hansen, T. F. (1997). Stabilizing selection and the comparative analysis of adaptation. *Evolution*, 51(5):1341–1351.

Climatic adaptation in underground organs

- 432 Howard, C. C., Folk, R. A., Beaulieu, J. M., and Cellinese, N. (2019). The monocotyledonous underground: global climatic and
433 phylogenetic patterns of geophyte diversity. *American Journal of Botany*, 106(6):850–863.
- 434 Howard, C. C., Tribble, C. M., Martínez-Gómez, J., Sessa, E. B., Specht, C. D., and Cellinese, N. (2021). 1, 2, 3, go! venture beyond gene
435 ontologies in plant evolutionary research. *American Journal of Botany*, 108(3):361–365.
- 436 Huelsenbeck, J. P., Nielsen, R., and Bollback, J. P. (2003). Stochastic mapping of morphological characters. *Systematic Biology*, 52(2):131–
437 158.
- 438 Iles, W. J., Smith, S. Y., Gandolfo, M. A., and Graham, S. W. (2015). Monocot fossils suitable for molecular dating analyses. *Botanical*
439 *Journal of the Linnean Society*, 178(3):346–374.
- 440 Janzen, D. H. et al. (1975). *Ecology of plants in the tropics*. Edward Arnold Publishers Ltd.
- 441 Kamenetsky, R. and Okubo, H. (2012). *Ornamental geophytes: from basic science to sustainable production*. CRC press.
- 442 Katoh, K. and Standley, D. M. (2013). MAFFT multiple sequence alignment software version 7: improvements in performance and
443 usability. *Molecular Biology and Evolution*, 30(4):772–780.
- 444 Kubitzki, K. and Huber, H. (1998). *Flowering plants, monocotyledons: Liliales (except Orchidaceae)*. Springer.
- 445 Lee, D.-C. and Bryant, H. N. (1999). A reconsideration of the coding of inapplicable characters: assumptions and problems. *Cladistics*,
446 15(4):373–378.
- 447 Leebens-Mack, J. (2020). Personal communication.
- 448 Maddison, W. P., Midford, P. E., and Otto, S. P. (2007). Estimating a binary character's effect on speciation and extinction. *Systematic*
449 *Biology*, 56(5):701–710.
- 450 Maitner, B. S., Boyle, B., Casler, N., Condit, R., Donoghue, J., Durán, S. M., Guaderrama, D., Hinchliff, C. E., Jørgensen, P. M., Kraft,
451 N. J., et al. (2018). The bien r package: A tool to access the Botanical Information and Ecology Network (BIEN) database. *Methods*
452 *in Ecology and Evolution*, 9(2):373–379.
- 453 May, M. R. and Moore, B. R. (2020). A bayesian approach for inferring the impact of a discrete character on rates of continuous-
454 character evolution in the presence of background-rate variation. *Systematic biology*, 69(3):530–544.
- 455 Miller, M. A., Pfeiffer, W., and Schwartz, T. (2011). The cypres science gateway: a community resource for phylogenetic analyses. In
456 *Proceedings of the 2011 TeraGrid Conference: extreme digital discovery*, pages 1–8.
- 457 Mirarab, S., Nguyen, N., Guo, S., Wang, L.-S., Kim, J., and Warnow, T. (2015). PASTA: ultra-large multiple sequence alignment for
458 nucleotide and amino-acid sequences. *Journal of Computational Biology*, 22(5):377–386.
- 459 Nielsen, R. (2002). Mapping mutations on phylogenies. *Systematic Biology*, 51(5):729–739.
- 460 Paradis, E. and Schliep, K. (2019). ape 5.0: an environment for modern phylogenetics and evolutionary analyses in R. *Bioinformatics*,
461 35(3):526–528.
- 462 Parsons, R. and Hopper, S. D. (2003). Monocotyledonous geophytes: comparison of south-western Australia with other areas of
463 mediterranean climate. *Australian Journal of Botany*, 51(2):129–133.

Climatic adaptation in underground organs

- 464 Pate, J. S. and Dixon, K. W. (1982). *Tuberous, cormous and bulbous plants*. International Scholarly Book Services Inc.[distributor].
- 465 Patterson, T. B. and Givnish, T. J. (2002). Phylogeny, concerted convergence, and phylogenetic niche conservatism in the core Liliales:
466 insights from rbcL and ndhF sequence data. *Evolution*, 56(2):233–252.
- 467 Phillips, S. J. and Dudík, M. (2008). Modeling of species distributions with Maxent: new extensions and a comprehensive evaluation.
468 *Ecography*, 31(2):161–175.
- 469 Plummer, M., Best, N., Cowles, K., and Vines, K. (2006). CODA: convergence diagnosis and output analysis for MCMC. *R news*,
470 6(1):7–11.
- 471 R Core Team (2013). *R: A Language and Environment for Statistical Computing*. R Foundation for Statistical Computing, Vienna, Austria.
- 472 Rabosky, D. L. and Goldberg, E. E. (2015). Model inadequacy and mistaken inferences of trait-dependent speciation. *Systematic biology*,
473 64(2):340–355.
- 474 Raunkiaer, C. et al. (1934). The life forms of plants and statistical plant geography; being the collected papers of C. Raunkiaer. *The life*
475 *forms of plants and statistical plant geography; being the collected papers of C. Raunkiaer*.
- 476 Rees, A. (1989). Evolution of the geophytic habit and its physiological advantages. *Herbertia*, 45:104–110.
- 477 Revell, L. J. (2012). phytools: an R package for phylogenetic comparative biology (and other things). *Methods in ecology and evolution*,
478 3(2):217–223.
- 479 Ronquist, F., Teslenko, M., Van Der Mark, P., Ayres, D. L., Darling, A., Höhna, S., Larget, B., Liu, L., Suchard, M. A., and Huelsenbeck,
480 J. P. (2012). MrBayes 3.2: efficient Bayesian phylogenetic inference and model choice across a large model space. *Systematic biology*,
481 61(3):539–542.
- 482 Sanderson, M. J. (2002). Estimating absolute rates of molecular evolution and divergence times: a penalized likelihood approach.
483 *Molecular Biology and Evolution*, 19(1):101–109.
- 484 Sanso, A. M. and Xifreda, C. C. (2001). Generic delimitation between *Alstroemeria* and *Bomarea* (Alstroemeriaceae). *Annals of Botany*,
485 88(6):1057–1069.
- 486 Sosa, V., Cameron, K. M., Angulo, D. F., and Hernández-Hernández, T. (2016). Life form evolution in epidendroid orchids: ecological
487 consequences of the shift from epiphytism to terrestrial habit in *Hexalectris*. *Taxon*, 65(2):235–248.
- 488 Sosa, V. and Loera, I. (2017). Influence of current climate, historical climate stability and topography on species richness and endemism
489 in Mesoamerican geophyte plants. *PeerJ*, 5(6):e3932–20.
- 490 Stevens, P. F. et al. (2016). Angiosperm Phylogeny Website. Version 13. *Angiosperm Phylogeny Website. Version 13*.
- 491 Tarasov, S. (2019). Integration of anatomy ontologies and evo-devo using structured markov models suggests a new framework for
492 modeling discrete phenotypic traits. *Systematic biology*, 68(5):698–716.
- 493 Tarasov, S., Mikó, I., Yoder, M. J., and Uyeda, J. C. (2019). PARAMO: A pipeline for reconstructing ancestral anatomies using ontologies
494 and Stochastic mapping. *Insect Systematics and Diversity*, 3(6):1.

Climatic adaptation in underground organs

- 495 Tribble, C. M., Martínez-Gómez, J., Howard, C. C., Males, J., Sosa, V., Sessa, E. B., Cellinese, N., and Specht, C. D. (2021). Get the shovel:
496 morphological and evolutionary complexities of belowground organs in geophytes. *American Journal of Botany*, 108(3):372–387.
- 497 Uyeda, J. C. (2019). bayou Tutorial. <https://github.com/uyedaj/bayou/blob/master/tutorial.md>. Accessed: 2021-06-30.
- 498 Uyeda, J. C. and Harmon, L. J. (2014). A novel Bayesian method for inferring and interpreting the dynamics of adaptive landscapes
499 from phylogenetic comparative data. *Systematic biology*, 63(6):902–918.
- 500 Uyeda, J. C., Zenil-Ferguson, R., and Pennell, M. W. (2018). Rethinking phylogenetic comparative methods. *Systematic Biology*,
501 67(6):1091–1109.
- 502 Vaidya, G., Lohman, D. J., and Meier, R. (2011). SequenceMatrix: concatenation software for the fast assembly of multi-gene datasets
503 with character set and codon information. *Cladistics*, 27(2):171–180.
- 504 Vasconcelos, T., Boyko, J. D., and Beaulieu, J. M. (2021). Linking mode of seed dispersal and climatic niche evolution in flowering
505 plants. *Journal of Biogeography*.
- 506 WCSP (2020). World checklist of selected plant families, facilitated by the Royal Botanic Gardens, Kew. <http://wcsp.science.kew.org>.
507 [org](http://wcsp.science.kew.org). Accessed: 2017-09-04.
- 508 Whigham, D. F. (2004). Ecology of woodland herbs in temperate deciduous forests. *Annu. Rev. Ecol. Evol. Syst.*, 35:583–621.